Synthesis and Crystal Structure of [Co(CO)$_4$(H$_7$Si$_8$O$_{12}$)]. A New Type of Monosubstituted Octanuclear Silasesquioxane with a Silicon–Cobalt Bond†

Gion Calzaferri,[*,a] Roman Imhof[a] and Karl W. Törnroos[b]

[a] Institute of Inorganic and Physical Chemistry, University of Berne, CH-3000 Berne 9, Switzerland
[b] Structural Chemistry, Stockholm University, S-106 91 Stockholm, Sweden

Reaction of octacarbonyldicobalt [Co$_2$(CO)$_8$] with octahydrosilasesquioxane H$_8$Si$_8$O$_{12}$ in toluene leads to [Co(CO)$_4$(H$_7$Si$_8$O$_{12}$)], a new monosubstituted, octanuclear silasesquioxane with a silicon–cobalt bond. The product has been analysed by ^{1}H, ^{13}C, ^{29}Si NMR and IR spectroscopies, mass spectrometry and microanalysis. The crystal structure of [Co(CO)$_4$(H$_7$Si$_8$O$_{12}$)] has been determined by single-crystal X-ray diffraction and is compared with the structures of H$_8$Si$_8$O$_{12}$, [Co(CO)$_4$(SiCl$_3$)] and [Co(CO)$_4$(SiF$_3$)]. The H$_7$Si$_8$O$_{12}$ fragment exhibits structural distortions consistently around, and originating from the Si atom to which the Co(CO)$_4$ fragment binds. The remaining part of the cage essentially retains C_3 symmetry, but is, nevertheless, in principle closer to the ideal O_h symmetry for this type of cage, than is crystalline H$_8$Si$_8$O$_{12}$, for which a non-crystallographic molecular symmetry of T_h is present. The comparison of the structures of the Co(CO)$_4$ fragments shows that these are consistently distorted and deviate from ideal C_{3v} symmetry. The distortions are essentially of the same kind in the three compounds and differ only in magnitude. The Si–Co distance in [Co(CO)$_4$(H$_7$Si$_8$O$_{12}$)] is 2.285 Å. The experimental findings have been compared with extended-Hückel molecular orbital calculations. Interaction between the Co(d$_{z^2}$) and the Si(p$_z$) orbitals leads to the bond between the two fragments. Overlap population analysis indicates small but significant bonding interaction between Si and C$_{eq}$ and antibonding interaction between the Co and the nearest O(Si). Fractional molecular orbital analysis indicates that the electronic structure of [Co(CO)$_4$(H$_7$Si$_8$O$_{12}$)] consists of three parts: orbitals belonging only to one of the two fragments and orbitals shared by both fragments. The highest-occupied molecular orbital (HOMO) of [Co(CO)$_4$(H$_7$Si$_8$O$_{12}$)] consists of oxygen lone pairs localised on H$_7$Si$_8$O$_{12}$. The lowest-unoccupied molecular orbital (LUMO) is identical with the LUMO of Co(CO)$_4$ and the first electronic transitions observed in the near UV are of H$_7$Si$_8$O$_{12}$ (oxygen lone pair) to Co(CO)$_4$ fragment charge-transfer type.

Octahydrosilasesquioxane H$_8$Si$_8$O$_{12}$ is a member of the large class of silasesquioxanes of the type (RSiO$_{1.5}$)$_{2n}$, $n = 1, 2, 3$ etc., which has attained much interest in the last six years. These three-dimensional molecular silicon compounds are discussed viz. as precursors for SiO$_2$ deposition,[1] as 'building blocks' for the preparation of highly siliceous materials,[7a] as precursors to organolithic macromolecular compounds[2] or as starting molecules for new organosiliceous polymers.[3] They are used as models for silicon oxide surfaces on which metal catalysed reactions take place.[4] Recently, Tacke et al.[5] published a synthesis for aminoorganyl-substituted octasilasesquioxanes. Octahydrosilasesquioxane H$_8$Si$_8$O$_{12}$ can be prepared in good yields by the polycondensation of SiHCl$_3$ in a biphasic solution.[6] Five different types of Si–H substitution reactions under retention of the cage structure have been reported up to now.[7] We have found that platinum-catalysed hydrosilylation can be used to prepare pure monosubstituted octanuclear hydrosilasesquioxanes of the type RH$_7$Si$_8$O$_{12}$ (R = alkyl, aryl or ferrocenyl)[8] and we now describe a new type of Si–H substitution, a reaction between H$_8$Si$_8$O$_{12}$ and [Co$_2$(CO)$_8$], which leads to the formation of the first monosubstituted hydrosilasesquioxane with a silicon–metal bond [Co(CO)$_4$-(H$_7$Si$_8$O$_{12}$)] [equation (1)].

The crystal structure of the new compound [Co(CO)$_4$(H$_7$-Si$_8$O$_{12}$)] is reported and related to that of H$_8$Si$_8$O$_{12}$, which has
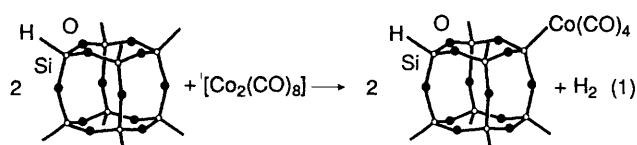
been reinvestigated recently.[9] The crystal structure as well as the electronic structure of [Co(CO)$_4$(H$_7$Si$_8$O$_{12}$)] may be seen as composed of two characteristic fragments, H$_7$Si$_8$O$_{12}$ and Co(CO)$_4$, and will be discussed in detail.

Results and Discussion

Synthesis.—Octahydrosilasesquioxane H$_8$Si$_8$O$_{12}$ was dissolved in toluene at 50 °C under CO and stirred together with octacarbonyldicobalt overnight. After evaporation of the solvent the crude brown material was separated on a size-exclusion liquid chromatography column. The white product was recrystallised from hexane–dichloromethane to give clear, colourless flakes.

Octacarbonyldicobalt [Co$_2$(CO)$_8$] reacts readily at room temperature with silanes [equation (2)].[10]

$$2\,\text{SiHR}_3 + [\text{Co}_2(\text{CO})_8] \longrightarrow 2\,[\text{Co(CO)}_4(\text{SiR}_3)] + \text{H}_2 \quad (2)$$
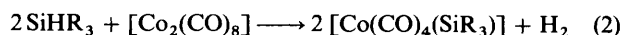
This type of hydrogen elimination accompanied by the cleavage of a metal–metal bond is common in organometallic chemistry and many of the known Si–Co(CO)$_4$ compounds
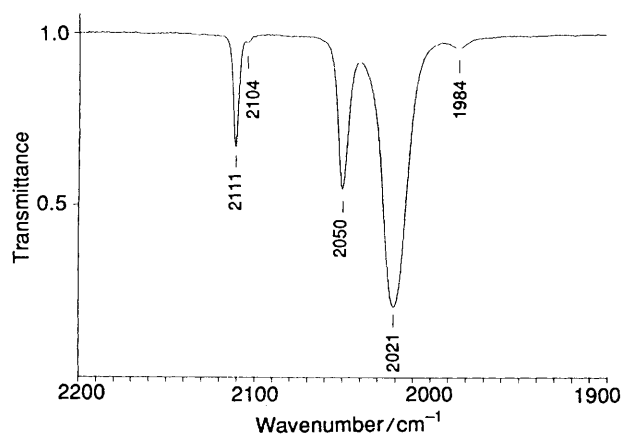
Fig. 1 Carbonyl stretching vibrations $v(CO)$ in the IR transmission spectrum of $[Co(CO)_4(H_7Si_8O_{12})]$ measured in CCl_4 with a resolution of $1\ cm^{-1}$

can be synthesised by applying this reaction.[11] Compared to the other known synthetic procedures we have to work above room temperature. This is a compromise between the low solubility of $H_8Si_8O_{12}$ at room temperature and the tendency of octacarbonyldicobalt to decompose at elevated temperature. Sommer and Lyons[12] have shown that the substitution of an H atom in Si–H compounds by $Co(CO)_4$ takes place with retention of the configuration at silicon.[12] Based on the cage structure of $[Co(CO)_4(H_7Si_8O_{12})]$, we assume that the mechanism of the reaction in equation (1) proceeds *via* five-co-ordinated silicon similar to the reaction path for the palladium-catalysed deuterium exchange of $H_8Si_8O_{12}$ to $D_8Si_8O_{12}$.[13]

Spectroscopy.—The IR transmission spectrum of $[Co(CO)_4$-$(H_7Si_8O_{12})]$ measured in CCl_4 (Fig. 1) shows in the region of the C–O stretching vibration three well distinguished symmetrical bands at 2111, 2050 and 2021 cm^{-1}. This splitting pattern is in agreement with C_{3v} symmetry and assignment of the three bands as an A_1 and an E mode for the three equatorial CO groups (2111 and 2021 cm^{-1}) and an A_1 mode for the apical CO group (2050 cm^{-1}) is straightforward. The two small bands at 2104 and 1984 cm^{-1} are ^{13}C-isotope bands of the equatorial CO groups.[14]

The ^1H NMR spectrum shows the expected splitting pattern with two singlets for the Si–H protons with relative intensities of 4:3. The ^{13}C NMR spectrum shows only one band, which means that the apical and the three equatorial CO groups are equivalent at room temperature. This is in agreement with the reported intramolecular rearrangement of the four CO ligands for comparable molecules.[15] The ^{29}Si NMR spectrum shows four signals with relative intensities of 1:3:1:3. The silicon, which is directly bound to the cobalt is shifted by about 40 ppm to lower field, as reported for other Si–$Co(CO)_4$ containing molecules.[16]

Molecular Structure.—The crystal structure of [Co-$(CO)_4(H_7Si_8O_{12})]$ with atomic labelling and anisotropic thermal parameters at the 50% probability level is shown in Fig. 2. Atomic coordinates and bond lengths and angles are given in Tables 1 and 2 respectively. The [Co(CO)₄-$(H_7Si_8O_{12})]$ molecule may be seen as composed of two characteristic fragments: the $H_7Si_8O_{12}$ cage and the $Co(CO)_4$ group. This allows us at first to compare the structure of each fragment separately with analogous fragments already known from the literature, and thereafter to analyse the structural consequences of the formation of the $[Co(CO)_4(H_7Si_8O_{12})]$ molecule. We choose as our reference compound for the cage fragment the crystal structure of $H_8Si_8O_{12}$, determined
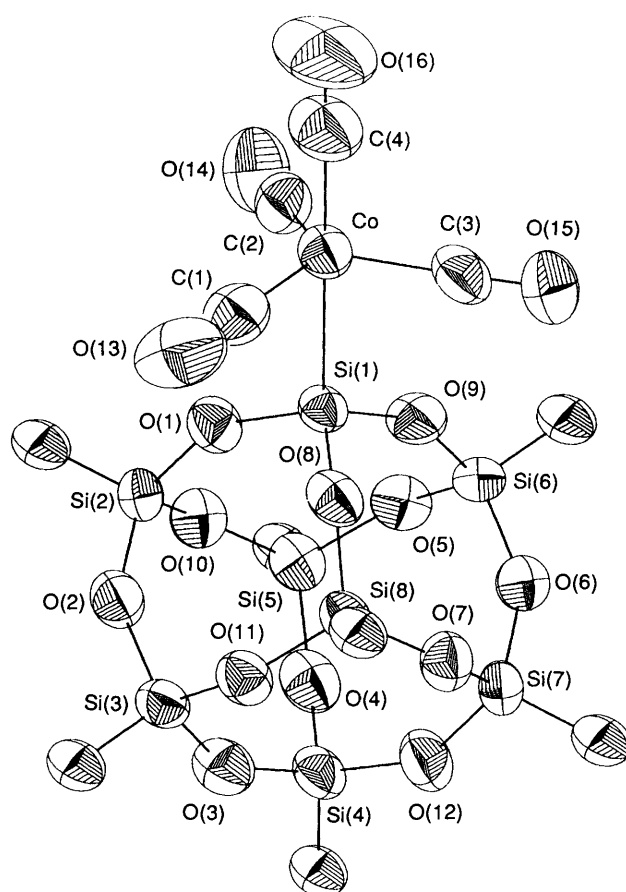

Fig. 2 The crystal structure of $[Co(CO)_4(H_7Si_8O_{12})]$, displayed with atomic labelling and anisotropic thermal parameters at the 50% probability level

Table 1 Atomic fractional coordinates for $[Co(CO)_4(H_7Si_8O_{12})]$ with estimated standard deviations in parentheses

Atom	x	y	z
Co	−0.250 66(9)	1.168 81(9)	0.424 14(3)
Si(1)	−0.393 07(15)	1.020 65(16)	0.313 59(6)
Si(2)	−0.799 05(16)	0.888 48(17)	0.264 34(7)
Si(3)	−0.727 41(17)	0.532 91(16)	0.204 25(7)
Si(4)	−0.730 50(17)	0.676 78(18)	0.050 31(7)
Si(5)	−0.803 36(16)	1.034 59(17)	0.110 06(7)
Si(6)	−0.399 83(16)	1.161 20(15)	0.156 82(6)
Si(7)	−0.325 99(17)	0.804 84(17)	0.097 32(7)
Si(8)	−0.320 72(15)	0.663 17(15)	0.251 88(7)
O(1)	−0.604 7(4)	0.976 7(4)	0.309 8(2)
O(2)	−0.799 7(4)	0.683 5(4)	0.246 8(2)
O(3)	−0.768 5(4)	0.558 7(4)	0.116 3(2)
O(4)	−0.799 9(4)	0.860 8(4)	0.059 9(2)
O(5)	−0.609 9(4)	1.154 6(4)	0.125 0(2)
O(6)	−0.328 9(4)	1.010 4(3)	0.114 2(2)
O(7)	−0.269 7(4)	0.717 6(4)	0.174 7(2)
O(8)	−0.319 9(4)	0.837 5(4)	0.302 7(2)
O(9)	−0.364 4(4)	1.134 4(4)	0.244 5(2)
O(10)	−0.849 2(4)	0.980 3(4)	0.188 0(2)
O(11)	−0.515 4(4)	0.547 2(4)	0.234 4(2)
O(12)	−0.520 2(4)	0.712 4(4)	0.053 6(2)
O(13)	−0.321 1(8)	0.828 2(7)	0.480 7(3)
O(14)	−0.527 2(6)	1.392 6(6)	0.393 8(3)
O(15)	−0.045 1(6)	1.254 4(6)	0.350 0(3)
O(16)	−0.069 1(9)	1.351 7(7)	0.568 1(3)
C(1)	−0.295 5(8)	0.959 4(8)	0.458 5(3)
C(2)	−0.421 4(8)	1.304 4(8)	0.404 3(3)
C(3)	−0.069 9(7)	1.219 0(7)	0.378 9(3)
C(4)	−0.138 1(9)	1.281 6(9)	0.512 7(3)

Table 2 Interatomic distances (Å) and angles (°) for $[Co(CO)_4(H_7Si_8O_{12})]$

Co–C(1)	1.784(6)	Si(2)–O(2)	1.609(3)	Si(5)–O(4)	1.611(3)	Si(7)–O(12)	1.609(3)
Co–C(2)	1.793(6)	Si(2)–O(10)	1.604(3)	Si(5)–O(5)	1.620(3)	Si(8)–O(7)	1.614(3)
Co–C(3)	1.787(6)	Si(3)–O(2)	1.609(3)	Si(5)–O(10)	1.611(3)	Si(8)–O(8)	1.612(3)
Co–C(4)	1.809(6)	Si(3)–O(3)	1.614(3)	Si(6)–O(5)	1.608(3)	Si(8)–O(11)	1.613(3)
Co–Si(1)	2.285(1)	Si(3)–O(11)	1.612(3)	Si(6)–O(6)	1.606(3)	C(1)–O(13)	1.121(6)
Si(1)–O(1)	1.620(3)	Si(4)–O(3)	1.605(3)	Si(6)–O(9)	1.610(3)	C(2)–O(14)	1.131(6)
Si(1)–O(8)	1.622(3)	Si(4)–O(4)	1.610(3)	Si(7)–O(6)	1.616(3)	C(3)–O(15)	1.141(6)
Si(1)–O(9)	1.616(3)	Si(4)–O(12)	1.608(3)	Si(7)–O(7)	1.609(3)	C(4)–O(16)	1.129(6)
Si(2)–O(1)	1.610(3)						
C(1)–Co–C(2)	120.5(3)	O(8)–Si(1)–O(9)	107.8(2)	O(5)–Si(5)–O(10)	109.8(2)	Si(4)–O(4)–Si(5)	150.3(2)
C(1)–Co–C(3)	120.8(3)	O(9)–Si(1)–Co	111.0(1)	O(5)–Si(6)–O(6)	109.7(2)	Si(5)–O(5)–Si(6)	145.4(2)
C(2)–Co–C(3)	115.2(3)	O(1)–Si(2)–O(2)	109.6(2)	O(5)–Si(6)–O(9)	109.1(2)	Si(6)–O(6)–Si(7)	148.9(2)
C(1)–Co–C(4)	96.4(3)	O(1)–Si(2)–O(10)	109.6(2)	O(6)–Si(6)–O(9)	110.1(2)	Si(7)–O(7)–Si(8)	147.4(2)
C(2)–Co–C(4)	96.1(3)	O(2)–Si(2)–O(10)	109.7(2)	O(6)–Si(7)–O(7)	109.1(2)	Si(1)–O(8)–Si(8)	149.7(2)
C(3)–Co–C(4)	96.0(3)	O(2)–Si(3)–O(3)	109.4(2)	O(6)–Si(7)–O(12)	109.7(2)	Si(1)–O(9)–Si(6)	151.3(2)
C(1)–Co–Si(1)	82.3(3)	O(2)–Si(3)–O(11)	109.2(2)	O(7)–Si(7)–O(12)	109.9(2)	Si(2)–O(10)–Si(5)	149.6(2)
C(2)–Co–Si(1)	84.7(3)	O(3)–Si(3)–O(11)	109.0(2)	O(7)–Si(8)–O(8)	109.1(2)	Si(3)–O(11)–Si(8)	149.3(2)
C(3)–Co–Si(1)	84.6(3)	O(3)–Si(4)–O(4)	109.4(2)	O(7)–Si(8)–O(11)	109.2(2)	Si(4)–O(12)–Si(7)	147.8(2)
C(4)–Co–Si(1)	178.7(3)	O(3)–Si(4)–O(12)	109.7(2)	O(8)–Si(8)–O(11)	110.2(2)	O(13)–C(1)–Co	179.0(5)
O(1)–Si(1)–Co	110.4(1)	O(4)–Si(4)–O(12)	108.9(2)	Si(1)–O(1)–Si(2)	148.7(2)	O(14)–C(2)–Co	177.9(5)
O(1)–Si(1)–O(8)	107.8(2)	O(4)–Si(5)–O(5)	109.1(2)	Si(2)–O(2)–Si(3)	148.3(2)	O(15)–C(3)–Co	178.7(5)
O(1)–Si(1)–O(9)	108.3(2)	O(4)–Si(5)–O(10)	109.2(2)	Si(3)–O(3)–Si(4)	147.6(2)	O(16)–C(4)–Co	179.5(5)
O(8)–Si(1)–Co	111.5(1)						

at 100 K.[9] This compound has a crystallographic symmetry of C_{3i}, but shows an effective molecular symmetry of T_h, thus still deviating from its ideal symmetry, O_h. In solution the ideal symmetry O_h is fulfilled as can be seen in the IR solution spectrum of $H_8Si_8O_{12}$. The symmetry reduction can, however, be seen in the Fourier-transform (FT) Raman spectrum of crystalline $H_8Si_8O_{12}$, where a splitting of the bands belonging to Si–H according to S_6 has been observed.[17] This deviation from O_h symmetry ensues from the departure of the oxygen atoms from the body-diagonal planes of the almost ideal silicon atom cube [the difference between the Si · · · Si body diagonals is a mere 0.009(1) Å in $H_8Si_8O_{12}$]. A direct measure of the deviation are the two distances between opposite oxygens, O(1,5)-distances, across the faces of the cube, which differ by 0.307(1) Å in $H_8Si_8O_{12}$. In the case of $[Co(CO)_4(H_7Si_8O_{12})]$ we are dealing with a molecular symmetry of C_1 and may strictly speaking face a more complex pattern of distortions due to the significantly larger number of degrees of freedom. The O(1,5)-deviations in the cage of $[Co(CO)_4(H_7Si_8O_{12})]$ are nevertheless considerably less, on average 0.126(6) Å, with minimum and maximum values being 0.098(6) and 0.231(6) Å. Consequently, the departure of the oxygen atoms out of the body-diagonal planes in the silicon cube is on average only 0.042(3) Å, the corresponding value in $H_8Si_8O_{12}$ being 0.112(1) Å. The only deformations in the $H_7Si_8O_{12}$ cage which significantly exceed those in $H_8Si_8O_{12}$ concern the Si · · · Si body-diagonal distances and the tetrahedral geometry of the silicon atom, Si(1), that binds to the $Co(CO)_4$ group. The unusually large body-diagonal distance for Si(1) · · · Si(4) of 5.411(2) Å in $[Co(CO)_4(H_7Si_8O_{12})]$ is surely an effect of the angular distortions around Si(1) caused by its bond to the $Co(CO)_4$ group. The remaining body-diagonal distances are Si(3) · · · Si(6) 5.373(2), Si(2) · · · Si(7) 5.359(2) and Si(5) · · · Si(8) 5.357 Å, the average for all four distances is 5.375(2) Å, to be compared to an average of 5.386(1) Å in $H_8Si_8O_{12}$. Small but systematic differences occur between the two structures for distances and angles of bonded atoms. Their mean values within the cage of $H_7Si_8O_{12}$ are as follows: Si–O 1.612(3) Å, Si–O–Si 148.7(2), O–Si–O 109.25(2)°; the average O–Si–O angle excluding the angles around Si(1) is 109.44(18)° compared with the average angle of 109.50(5)° in $H_8Si_8O_{12}$. The O–Si(1)–O angles average 107.9(2)°, but the Si–O distances and the Si–O–Si angles involving Si(1) do not deviate much from the rest of the cage, indicating that the Si(1) atom is

actually pushed out of the cage, resulting in the abnormal Si · · · Si body-diagonal distance. It is obvious that the remaining tetrahedral angles are well conserved close to the ideal value. The larger flexibility lies instead in the softer Si–O–Si angles, α, which nicely follow the relationship (3) derived for the spherosilasesquioxanes.[18]

$$d(\text{Si–O})/\text{Å} = 1.59 + [2.1 \times 10^{-8} (180 - \alpha)^4] \quad (3)$$

The average Si–O distance in $[Co(CO)_4(H_7Si_8O_{12})]$ is smaller than that in $H_8Si_8O_{12}$, 1.618(1) Å, for which equation (3) gives a smaller average Si–O–Si angle of 147.55(7)°. Along the Si(1) · · · Si(4) body diagonal a C_3 symmetry is still preserved in the $H_7Si_8O_{12}$ cage in conformity with the essentially cubic arrangement of the silicon atoms. Due to the distortions of the Si(1) tetrahedron, the inversion centre in the cage is obviously lost. The edge of the Si · · · Si cube is on average 3.103(2) Å, the corresponding distance in the $H_8Si_8O_{12}$ molecule being practically the same at 3.108(6) Å. It was shown for $H_8Si_8O_{12}$, that such a molecule with an ideal O_h symmetry, assuming the O–Si–O angle to be 109.5° and considering the observed mean Si–O distance, requires the Si–O–Si angle to be 148.4°.[9] Thus in principle the $H_7Si_8O_{12}$ cage comes closer to the ideal O_h symmetry than does $H_8Si_8O_{12}$, if we consider its less strained mean Si–O–Si angle of 148.7(2)° and the much smaller deviation of the oxygen atoms from the body-diagonal planes of the Si_8 cube, and if we disregard the O–Si(1)–O angular distortions.

The $Co(CO)_4$ group deviates significantly from C_{3v} symmetry and subsequently the five-co-ordinate metal structure, Si–Co–$(CO)_4$, is a distorted trigonal bipyramid. The main distortion lies in the differing angles between the equatorial carbon atoms, in that two of these are similar, 120.7(3)° on average, but the third is only 115.2(3)°. The equatorial carbonyls bend out of the basal plane towards Si(1) with a mean angle C_{eq}–Co–Si(1) of 83.9(2)°, the mean opposite angle C_{eq}–Co–C(4) being 96.2(2)°. As a consequence of this, Co is displaced out of the carbon equatorial plane by 0.192(3) Å. The equatorial carbonyl group C(1)–O(13) lies closer to Si(1), 2.703(6) Å for C(1), in comparison with the two other equatorial carbonyls, which are almost equally distant from Si(1) with a mean value of 2.769(5) Å. The corresponding angles C_{eq}–Co(1)–Si(1) are 82.3(3)° for C(1) but 84.7(3) and 84.6(3)° for C(2) and C(3). The apical Co–C(4) bond length, 1.809(6) Å, is slightly but

Table 3 Comparison of distances (Å) and angles (°) in $[Co(CO)_4(H_7Si_8O_{12})]$ and $[Co(CO)_4(SiX_3)]$ (X = F or Cl)

Compound	$[Co(CO)_4(H_7Si_8O_{12})]$	$[Co(CO)_4(SiCl_3)]$	$[Co(CO)_4(SiF_3)]$
Co–Si	2.285(1)	2.254(3)	2.226(5)
Co–C_{ap}	1.809(6)	1.797(9)	1.80(2)
C–O_{ap}	1.128(8)	1.136(8)	1.13(2)
Co–C_{eq} (av.)	1.788(6)	1.767(9)	1.78(1)
C–O_{eq} (av.)	1.131(8)	1.151(8)	1.12(1)
Si–C_{eq} (av.)	2.747(6)	2.746(9)	2.74(2)
Co–Si–X (av.)	111.0(1) (X = O)	113.3(1) (X = Cl)	114.6(5) (X = F)
X–Si–X (av.)	107.7(2)	105.4(2)	103.6(8)
C_{eq}–Co–Si–X (av.)	73.3(2)	62.8(4)	61.0(6)
Si–Co–C_{eq} (av.)	83.9(2)	85.2(3)	85.6(6)
C_{eq}–Co–C_{ap} (av.)	96.2(3)	94.8(4)	94.4(8)
Co–$(CO)_{eq}$ (av.)	178.5(2)	179.2(9)	179.5(11)
C_{eq}–Co–C_{eq} (av.)	118.9(3)	119.3(9)	119.4(7)
C_{eq}–Co–C_{eq} (min.)	115.2(3)	117.0(9)	117.3(7)
C_{eq}–Co–C_{eq} (max.)	120.8(3)	123.5(9)	120.5(4)
Co–$(CO)_{ap}$	179.5(7)	177.1(9)	176.8(18)
Si–Co–C_{ap}	178.7(2)	177.2(9)	178.4(18)

significantly longer than the corresponding ones in the equatorial plane, which are rather similar with a mean value of 1.788(6) Å. The C–O distances are, however, essentially the same for all four carbonyls, the mean being 1.131(8) Å.

Crystal-structure reports containing Si–Co bonds are scarce, but include trichloro-[19] and trifluoro-silyltetracarbonylcobalt,[20] which are closely related to $[Co(CO)_4(H_7Si_8O_{12})]$. A comparison between $[Co(CO)_4(H_7Si_8O_{12})]$ and these structures is compiled in Table 3. It is noteworthy how similar the $Co(CO)_4$ groups are in the three structures. The significant differences that do appear concern the Si–Co bond distance, the bending angle of the equatorial CO groups towards Si(1) and the degree of staggering. Major angular distortions in the silicon tetrahedron are apparent for all three structures and are the clearest consequence of the interaction between the silyl and the $Co(CO)_4$ group. The staggered orientation is almost optimal for $[Co(CO)_4(SiCl_3)]$ and $[Co(CO)_4(SiF_3)]$ but in the case of $[Co(CO)_4(H_7Si_8O_{12})]$, the deviation from the optimum position is about 13°. Modified extended-Hückel molecular orbital (EHMO) calculations in the ASED form (atom superposition and electron delocalisation) discussed in the next section result in a minimum O–Si–Co–C_{eq} angle of 60° with a small rotational barrier of 0.2 eV. We therefore conclude that the observed deviation is caused by crystal-packing effects. The distance Si–C_{eq} is the same in all structures, and the angles C_{eq}–Co–Si in $[Co(CO)_4(H_7Si_8O_{12})]$ thus adapt to the increased Si–Co distance by decreasing in magnitude.

The packing of the molecules in the crystal as illustrated in Fig. 3 exhibit the $Co(CO)_4$ groups clustered together around the centre of the unit cell, while the $H_7Si_8O_{12}$ cages gather at the ends of the unit cell in a displaced face-to-face arrangement.

This orientation of the cages produces four short O ••• Si intermolecular contacts, 3.541(3) Å for O(5¹) ••• Si(3) (1 x, y − 1, z) and 3.572(3) Å for O(11ᴵᴵ) ••• Si(6) (II, x, y + 1, z), per molecule, passing through the crystal approximately along the b axis, with the associated angles O ••• Si–O averaging 170.5(2)°. Such contacts are numerous also in the structure of $H_8Si_8O_{12}$, and are interpreted as particularly favourable for a nucleophilic attack by the oxygen atom on the silicon atom.[9]

Molecular Orbital Calculations.—The modified extended-Hückel formalism (EHMO) in its ASED (atom superposition and electron delocalisation) form is able to describe experimental geometries of organic and organometallic molecules.[13,21] From our study of the electronic structure of $H_8Si_8O_{12}$ we know that the oxygen lone pairs, which form the highest occupied molecular orbital (HOMO) in this compound, appear at about 10.7 eV.[13] The first ionisation energy of H_2O is
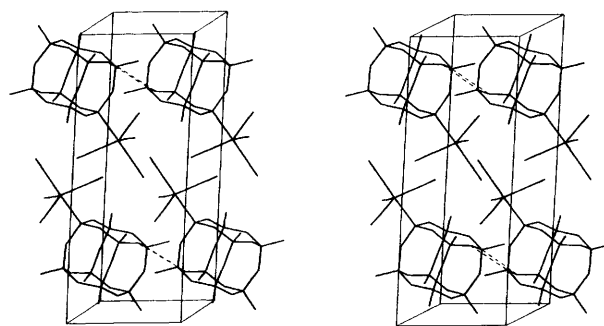

Fig. 3 Stereoscopic illustration of the molecular packing of $[Co(CO)_4(H_7Si_8O_{12})]$; intermolecular O ••• Si contacts are indicated with dashed lines

observed at 12.6 eV and attributed to the p-type oxygen lone pair, and the first ionisation potential of the CO molecule appears at about 14 eV. The electronic structure of $[Co(CO)_4(H_7Si_8O_{12})]$ is expected to be a superposition of that of the $H_7Si_8O_{12}$ and the $Co(CO)_4$ fragments. To what extent does the Si–Co bond influence the properties of each of these fragments? What is new in the electronic structure of $[Co(CO)_4(H_7Si_8O_{12})]$? The nature of the Si–Co bond of $[Co(CO)_4(SiX_3)]$ (X = F or Cl) has been discussed several years ago.[22] To model the energy hypersurface E [d(Si–Co), d(Co–C)] we have optimised the κ(Si–Co) and κ(Co–C) parameters to reproduce these two experimental bond lengths. As an important result we have found that the general form of the hypersurface shown in Fig. 4 is not affected by these two parameters within a large range of κ values. The same is true for the electronic structure. Only the position of the minimum of E[d(Si–Co), d(Co–C)] is shifted. After this first check all calculations have been carried out with the parameters reported in Table 5.

Two main features are observed in Fig. 4. The first is that the Si–Co and the Co–C stretching modes are not coupled. This means that lengthening or shortening of one bond does not affect the other. This explains why the average Co–C distances in the three molecules are within 0.02 Å of each other. The significant lengthening of the Si–Co bond distance from $[Co(CO)_4(SiF_3)]$ to $[Co(CO)_4(H_7Si_8O_{12})]$ of about 0.06 Å is accompanied by a decrease of the Si–Co–C_{eq} bond angle. The second observation is that the Si–Co stretching mode is extremely soft. A change in d(Si–Co) of 0.05 Å costs only about 0.007 eV. From this we conclude that the small differences in the Si–Co lengths of the $[Co(CO)_4(SiX_3)]$ and $[Co(CO)_4(H_7$-

Si_8O_{12})] molecules cannot be modelled by our calculations. The Co–C stretching mode is stiffer but still soft. The IR spectrum shows several bands in the Co–C stretching vibration region at about 520 cm^{-1}. The assignment of these bands remains uncertain because normal-coordinate analysis of [Co(CO)$_4$(H$_7$-Si$_8$O$_{12}$)] has not yet been carried out. Based on the Co–C overlap population in Fig. 5, however, we expect the apical mode to appear at a somewhat lower frequency than the equatorial one. This is consistent with the larger Co–C$_{ap}$ bond distance in the crystal structure. The C–O overlap population of the apical CO group is larger than the equatorial one. In the H$_7$Si$_8$O$_{12}$ fragment we recognise that the Si–O bonds adjacent to the Co(CO)$_4$ fragment have a larger overlap population with respect to H$_8$Si$_8$O$_{12}$. In the crystal structure we observe a shortening of the mean Si–O distance with respect to H$_8$Si$_8$O$_{12}$
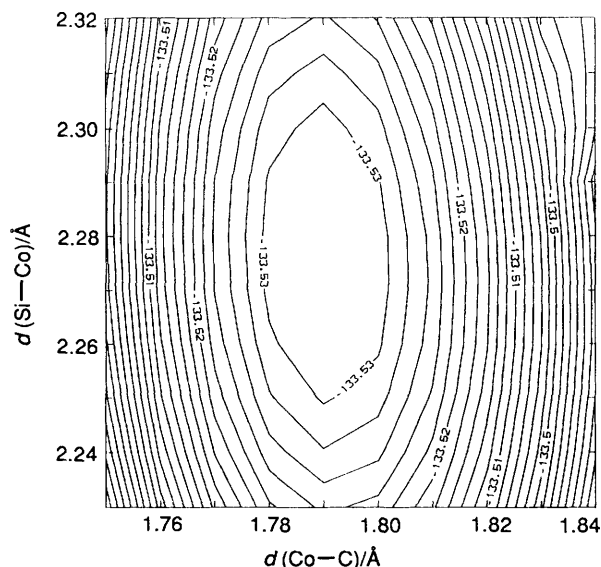

Fig. 4 Potential energy surface $E_{(tot)}$ of [Co(CO)$_4$(H$_7$Si$_8$O$_{12}$)] for the Si–Co and the Co–C stretching motion

from 1.618 to 1.612 Å. The small positive overlap populations between Si and C$_{eq}$ resembles an attractive interaction between these atoms. At the same time a negative overlap population between O(Si) and Co is observed whereas the interaction between O(Si) and C$_{eq}$ is negligible. These observations help us to understand why the observed O–Si–Co–C$_{eq}$ angle is smaller than 90°. The differences in the crystal structures of the three [Co(CO)$_4$(SiX$_3$)] molecules is the result of at least three factors, namely the direct Si–Co interaction, the interaction between Co and the ligand X and the attraction between Si and C$_{eq}$. We would like to add that the calculated charges on the H atoms are consistent with the 4:3 intensity pattern in the ^{1}H NMR spectrum.

The electronic structure of [Co(CO)$_4$(H$_7$Si$_8$O$_{12}$)] is easy to understand if we split it in three parts as shown in Fig. 6, which is the result of a fragment molecular orbital (FMO) calculation.[23] The orbitals localised on the H$_7$Si$_8$O$_{12}$ and on the Co(CO)$_4$ fragments are denoted by A and C, those delocalised over the whole molecule are denoted as B. The main correlations between the levels of the fragments and the delocalised molecular orbitals of region B are indicated with dotted lines. The orbitals of region B are responsible for the bonding and antibonding interactions between H$_7$Si$_8$O$_{12}$ and Co(CO)$_4$, and are illustrated in Fig. 7. It shows that the bond between the two fragments is simply the result of the interaction between the
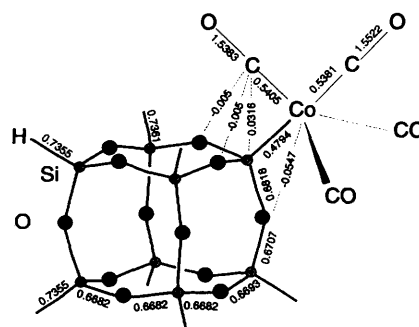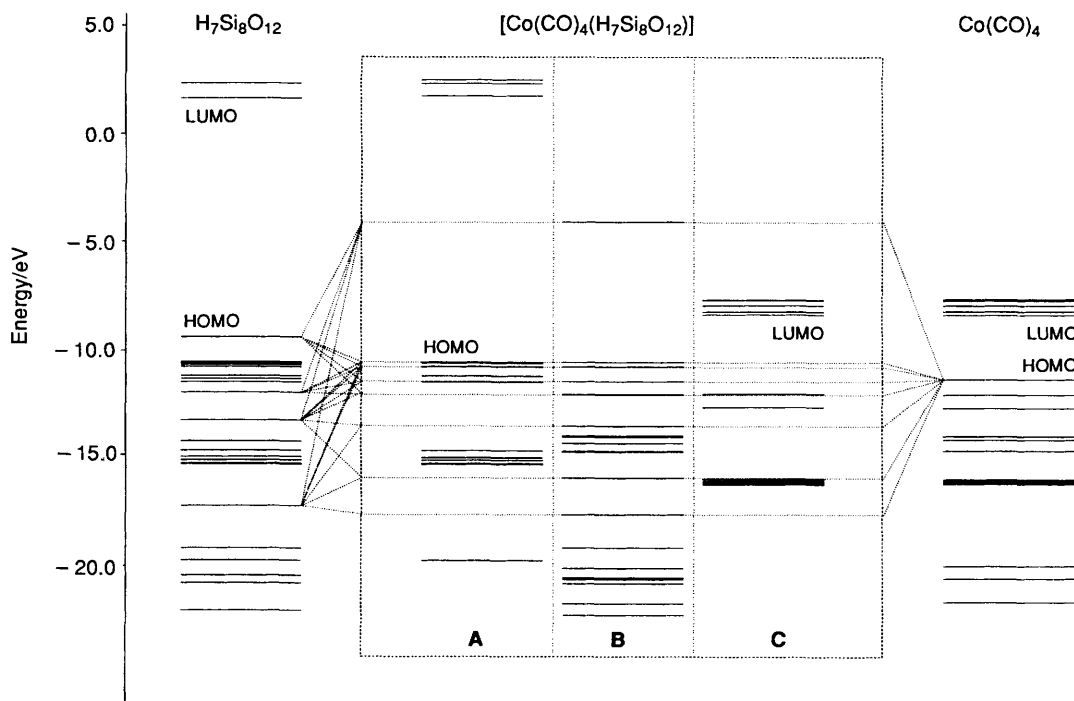

Fig. 5 Overlap population of [Co(CO)$_4$(H$_7$Si$_8$O$_{12}$)]

Fig. 6 Correlation diagram for H$_7$Si$_8$O$_{12}$ + Co(CO)$_4$ ⟶ [Co(CO)$_4$(H$_7$Si$_8$O$_{12}$)]. The energy levels of [Co(CO)$_4$(H$_7$Si$_8$O$_{12}$)] are split into three parts. Parts A and C contain the orbitals localised on the H$_7$Si$_8$O$_{12}$ and on the Co(CO)$_4$ fragment, respectively. The molecular orbitals of region B are delocalised over the whole molecule

Co(d_{z^2}) orbital and the Si(p_z) orbital. In addition to this the overlap population indicates a small but significant interaction between Co and O–(Si). Two groups of orbitals responsible for this are found in the HOMO region of [Co(CO)$_4$(H$_7$Si$_8$O$_{12}$)]. Only one of each group is sketched in Fig. 7. Essentially, it is an interaction between the Co(d_{z^2}) orbital and the O(p_z)(Si) orbitals. Another small contribution comes from the interaction between Si and the C$_{eq}$ atoms. At about -16 eV a first antibonding orbital of this type is found.

If we now try to understand the first electronic transitions of [Co(CO)$_4$(H$_7$Si$_8$O$_{12}$)] the situation appears to be too complicated because of the many closely lying levels in the HOMO and in the lowest-unoccupied molecular orbital (LUMO) region involved. Experimentally the UV/VIS spectrum measured in n-hexane at room temperature starts with a long tail at about 380 nm which develops after some weak shoulders to a first maximum below 200 nm. Since the HOMO region consists of oxygen lone-pair orbitals we can attribute the first electronic transitions to be of charge-transfer type in which an electron of the HOMO region A is transferred to the LUMO region C [equation (4)].

$$[H_7Si_8O_{12}][Co(CO)_4] \xrightarrow{h\nu} [H_7Si_8O_{12}]^+[Co(CO)_4]^- \quad (4)$$
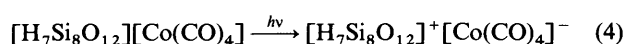
Individual oscillator strengths for the A to C charge-transfer transitions have been calculated to be at best 1.5×10^{-3}. The two highest occupied orbitals of region B belong mainly to the H$_7$Si$_8$O$_{12}$ fragment and are by 90% of oxygen lone pair character with some Co contribution. This means that the B to C transitions are of the same H$_7$Si$_8$O$_{12}$-(oxygen lone pair) to Co(CO)$_4$ fragment charge-transfer type. The individual oscillator strengths of this B to C charge-transfer transition, however, have been calculated to be up to 0.03.

Experimental

Chemicals.—Solvents were purchased from commercial sources and used as received. Octacarbonyldicobalt (Fluka) was also commercially available. Octahydrosilasesquioxane H$_8$Si$_8$O$_{12}$ was prepared according to the method of Agaskar[6] and recrystallised from hot cyclohexane.

Physical Methods.—High-performance liquid chromatography (HPLC) was performed with a Merck-Hitachi LC 6200 pump, an Erma ERC 3511 solvent degasser, an Erma ERC 7512 RI detector and a HP 3396A integrator. A 600 × 25 mm PolymerLab size-exclusion HPLC column (pore size 50 Å, particle size 10 m) was used. Hexane fraction (Romil Chemicals) was used as eluent. The flow rate was 6 cm^3 min^{-1} at room temperature. The ^{1}H, ^{13}C and ^{29}SiNMR spectra were recorded on a Bruker AC-300 instrument using CDCl$_3$ as solvent. The infrared transmission spectrum was measured in CCl$_4$ with a BOMEM DA3.01 FTIR spectrometer equipped with a liquid nitrogen cooled MCT detector (700–5000 cm^{-1}) and a KBr beamsplitter (450–4000 cm^{-1}) with a resolution of 1 cm^{-1}. The mass spectrum was recorded on a MAT-CH7A instrument. The elemental analysis was performed by the Analytical Department of Ciba-Geigy, Basel.

Synthesis.—The compound H$_8$Si$_8$O$_{12}$ (400 mg, 0.94 mmol) was dissolved in toluene (50 cm^3) at 50 °C under CO. Octacarbonyldicobalt (150 mg, 0.44 mmol) was added and the yellow solution was stirred for 15 h under CO at 50°C. After evaporation of the solvent a brown solid precipitated which was suspended in hexane fraction (Romil Chemicals), filtered and the remaining yellow-brown solution injected on a size-exclusion HPLC column. The crude white product was recrystallized from hexane–dichloromethane (1 : 1) to give clear, colourless flakes. The yield of [Co(CO)$_4$(H$_7$Si$_8$O$_{12}$)] was 56 mg (0.094 mmol, 10%) (Found: C, 8.55; H, 1.35; Co, 10.1; Si, 37.6. C$_4$H$_7$CoO$_{16}$Si$_8$ requires: C, 8.10; H, 1.20; Co, 9.90; Si, 37.80%). IR: ν_{max} 2275m, 2111s, 2104w, 2050s, 2021vs, 1984w, 1138vs, 1101s, 904w, 886vs, 881vs and 840m cm^{-1}. NMR (CDCl$_3$, standard SiMe$_4$): ^{1}H (300 MHz), δ 4.26 (s, 4 H) and 4.27 (s, 3 H); ^{13}C (75 MHz), δ 196.5; ^{29}Si (60 MHz, inverse gated, external standard), δ -46.04 (1 Si), -84.46 (3 Si), -84.62 (1 Si) and -86.35 (3 Si). Mass spectrum (70 eV): m/z 593 {30, $[M - 1]^+$}, 565 {33, $[M - 1 - CO]^+$}, 537 {29, $[M - 1 - 2CO]^+$}, 510 {100, $[M - 3CO]^+$}, 482 {77, $[M - 4CO]$}$^+$ and 423 {84%, $[M - Co(CO)_4]^+$}.

Crystal Structure Determination and Refinement.—Details of the experiment and refinement are given in Table 4. The crystals
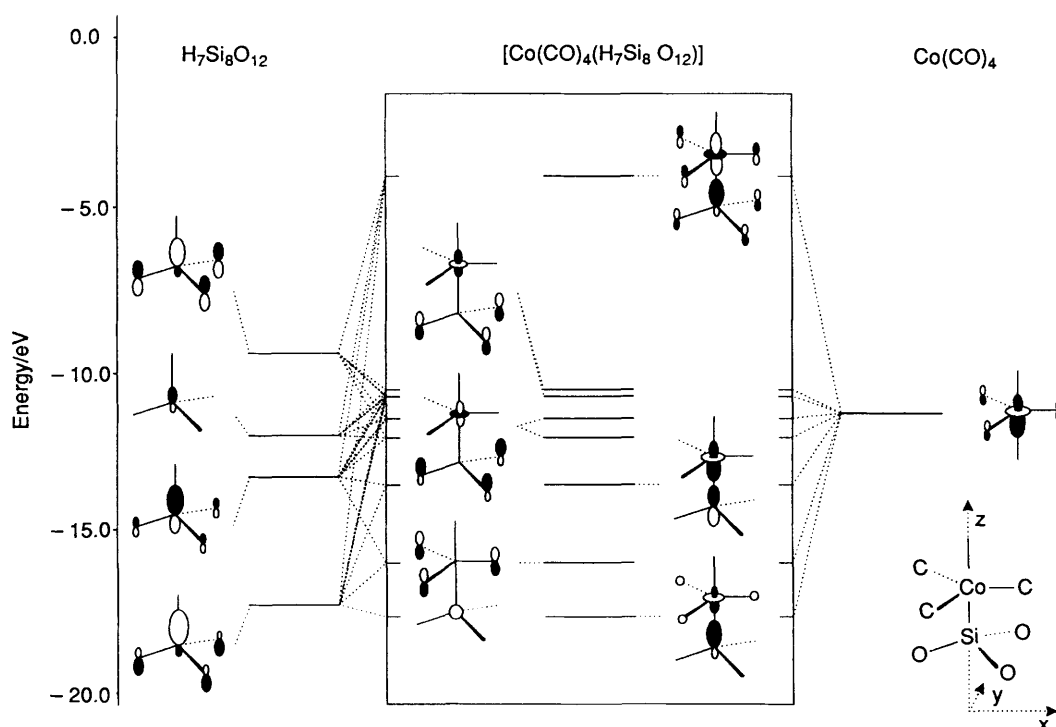

Fig. 7 Region B molecular orbitals of [Co(CO)$_4$(H$_7$Si$_8$O$_{12}$)] which are correlated in Fig. 6 to the orbitals of the two fragments

Table 4 Experimental data for the X-ray crystal structure analysis

Molecular formula	$C_4H_7CoO_{16}Si_8$
M	594.75
Crystal dimensions/mm	0.45 × 0.25 × 0.075
Crystal colour, shape	Colourless, transparent flakes
Crystal system	Triclinic
Space group	$P\bar{1}$
a/Å	7.7765(10)
b/Å	7.7565(10)
c/Å	18.457(3)
α/°	92.318(12)
β/°	102.130(11)
γ/°	97.923(20)
U/Å^3	1075.3(2)
T/K	291
Z	2
D_c/g cm^{-3}	1.837
Radiation type (λ/Å)	Mo-Kα (0.710 73)
μ(Mo-Kα)/mm^{-1}	1.313
Transmission factor range	0.7183–0.9071
$F(000)$	596
Scan type	ω–2θ
θ range/°	2.26–30.00
Index range	$-10 < h < 0, -10 < k < 10, -25 < l < 25$
No. of unique data	6243
No. of observed data $[F_o^2 > 3\sigma(F_o^2)]$	2144
Final R for observed data [a]	0.0292
Final R' for observed data [b]	0.0760
Goodness of fit, S [c]	1.092
Final difference-Fourier residuals, maximum and minimum/e Å^{-3}	0.28, -0.22
Largest and mean Δ/σ	0.000, 0.000

[a] $R = \Sigma||F_o| - |F_c||/\Sigma|F_o|$; conventional R value based on $F_o > 4\sigma(F_o)$ observation criterion. [b] $R' = \{\Sigma[w(F_o^2 - F_c^2)^2]/\Sigma[w(F_o^2)^2]\}^{\frac{1}{2}}$ where $w = 1/[\sigma^2(F_o^2) + (0.0470P)^2 + 0.30P]$, $P = [(F_o^2, 0)_{max} + 2F_c^2]/3$. [c] $S = \{\Sigma[w(F_o^2 - F_c^2)^2]/(n - p)\}^{\frac{1}{2}}$ where n is the number of observations and p the number of parameters.

Table 5 EHMO parameters

Atom	N	n_s	ζ_s	H_{ss}/eV	n_p	ζ_p	H_{pp}/eV
Si	4	3	1.600	-20.44	3	1.600	-12.41
O(Si)	6	2	2.575	-26.13	2	2.275	-10.80
H	1	1	1.300	-13.43			
Co	9	4	1.700	-9.51	4	1.050	-3.75
C	4	2	1.710	-21.83	2	1.625	-12.66
O(C)	6	2	2.575	-30.28	2	2.275	-14.14

	n_d	C_1	C_2	ζ_1	ζ_2	H_{dd}/eV
Co	3	0.555	0.646	5.550	1.900	-12.66

were rather thin and brittle flakes with irregular faces. A specimen was cut out of such a flake into a rectangular piece of suitable dimensions and mounted in a quartz capillary. The initial intention was to perform the experiment at low temperature, but repeated trials to cool the crystal proved unrealisable due to severe crystal cracking. This cracking might be caused by molecular movement or rearrangements taking place probably within the Co(CO)$_4$ group as a function of temperature.[15] Reflection data were collected on a STOE AED-2 four-circle instrument, using Mo-Kα radiation. Precise lattice parameters were determined from least-squares refinement of setting angles for 36 reflections. Crystal decay was monitored every 240 min using 6 reflections. The final decay amounted to 10.82%, and was corrected for by linear interpolation. Considering the unfavourable crystal shape an absorption correction was made, applying a Gaussian quadrature numerical method. The final agreement for equivalent reflections, R_{int}, was 0.0271. The structure was solved by fragment $(H_7Si_8O_{12})^9$ search in Patterson space using PATSEE[24] and SHELXS 86[25] in combination. Subsequent full-matrix least-squares refinement of a total of 270 parameters, with respect to $|F^2|$, was made with SHELXL 92,[26] refining anisotropic thermal parameters

for all non-hydrogen atoms. Hydrogen atom positions were geometrically idealised and the Si–H distance restrained to 1.460(5) Å, from the average Si–H distance found in a single-crystal neutron diffraction study of $H_8Si_8O_{12}$.[27] The isotropic thermal parameter of the hydrogens was refined in one variable common to all hydrogen atoms. Additional geometrical calculations were made with PLATON,[28] and the molecular illustrations with PEANUT[29] and SCHAKAL 92.[30]

Additional material available from the Cambridge Crystallographic Data Centre comprises H-atom coordinates, thermal parameters and remaining bond lengths and angles.

Molecular Orbital Calculations.—Molecular orbital calculations have been carried out by the extended Hückel method.[31] The off-diagonal elements were calculated as[32] $H_{ij} = 0.5\ KS_{ij}$- $(H_{ii} + H_{jj})$ with the distance dependent weighted formula[33] $K = 1 + \kappa e^{-\delta(R - R_o)}$ with $k = \kappa + \Delta^2 - \kappa\Delta^4$ and $\Delta = (H_{ii} - H_{jj})/(H_{ii} + H_{jj})$.

To correct for the core–core repulsion, a two-body term as explained in ref. 33 was taken into account. The computer program to perform this type of calculation is available from the QCPE.[34]

The parameters used are listed in Table 5 and were kept constant during all the calculations. The coulomb integrals H_{ii} for the $H_7Si_8O_{12}$ fragment were taken from the calculations on $H_8Si_8O_{12}$.[13] Those of the Co(CO)$_4$ fragment were obtained by charge iteration on the whole molecule [Co(CO)$_4$($H_7Si_8O_{12}$)]. Calculations have been carried out by assuming a simplified geometry, *i.e.* all d(Co–C) = 1.794 Å, d(C–O) = 1.131, α(Co–C–O) = 180°, α(O–Si–Co–C$_{eq}$) = 83.9° and the $H_7Si_8O_{12}$ fragment with bond lengths and angles equal to those of $H_8Si_8O_{12}$. Standard $\kappa = 1.0$ and $\delta = 0.35$ Å^{-1} were applied, with the exception of the Si–Co and Co–C bonds for which $\kappa = 0.82$ and 0.6 were used. Oscillator strengths have been calculated with the program EDiT[35] by applying the EHMO

wavefunctions. EDiT calculates all integrals involved in a rigorous way.

References

1 S. B. Desu, C. H. Peng, T. Shi and P. A. Agaskar, *J. Electrochem. Soc.*, 1992, **139**, 2682.

2 P. A. Agaskar, *Inorg. Chem.*, 1990, **29**, 1603.

3 D. Hoebbel, I. Pitsch and D. Heidemann, *Z. Anorg. Allg. Chem.*, 1991, **592**, 207.

4 F. J. Feher and R. L. Blanski, *Organometallics*, 1993, **12**, 958.

5 R. Tacke, A. Lopez-Mras, W. S. Sheldrick and A. Sebald, *Z. Anorg. Allg. Chem.*, 1993, **619**, 347.

6 P. A. Agaskar, *Inorg. Chem.*, 1991, **30**, 2702.

7 (*a*) V. W. Day, W. G. Klemperer, V. V. Mainz and D. M. Millar, *J. Am. Chem. Soc.*, 1985, **107**, 8262; (*b*) P. A. Agaskar, V. W. Day and W. G. Klemperer, *J. Am. Chem. Soc.*, 1987, **109**, 5554; (*c*) H. Bürgy and G. Calzaferri, *Helv. Chim. Acta*, 1990, **73**, 698; (*d*) D. Herren, H. Bürgy and G. Calzaferri, *Helv. Chim. Acta*, 1991, **74**, 24.

8 G. Calzaferri, D. Herren and R. Imhof, *Helv. Chim. Acta*, 1991, **74**, 1278; G. Calzaferri and R. Imhof, *J. Chem. Soc., Dalton Trans.*, 1992, 3391.

9 T. P. E. auf der Heyde, H. B. Bürgi, H. Bürgy and K. W. Törnroos, *Chimia*, 1991, **45**, 38.

10 J. F. Harrod and A. J. Chalk, *J. Am. Chem. Soc.*, 1965, **87**, 1133; B. J. Aylett and J. M. Campbell, *Chem. Commun.*, 1965, 217.

11 T. D. Tilley, in *The silicon–heteroatom bond*, eds. S. Patai and Z. Rappoport, Wiley, New York, 1991, ch. 9, pp. 245–307;

12 L. H. Sommer and J. E. Lyons, *J. Am. Chem. Soc.*, 1968, **90**, 4197.

13 G. Calzaferri and R. Hoffmann, *J. Chem. Soc., Dalton Trans.*, 1991, 917.

14 D. J. Darensbourg, *Inorg. Chim. Acta*, 1970, **4**, 597.

15 D. L. Lichtenberger and T. L. Brown, *J. Am. Chem. Soc.*, 1977, **99**, 8187.

16 R. Krentz and R. K. Pomeroy, *Inorg. Chem.*, 1985, **24**, 2976; S. Li, D. L. Johnson, J. A. Gladysz and K. L. Servis, *J. Organomet. Chem.*, 1979, **166**, 317.

17 M. Bärtsch, P. Bornhauser, H. Bürgy and G. Calzaferri, *Spectrochim. Acta, Part A*, 1991, **47**, 1627.

18 H. B. Bürgi, K. W. Törnroos, G. Calzaferri and H. Bürgy, *Inorg. Chem.*, in the press.

19 W. T. Robinson and J. Ibers, *Inorg. Chem.*, 1967, **6**, 1208.

20 K. Emerson, P. R. Ireland and W. T. Robinson, *Inorg. Chem.*, 1970, **9**, 436.

21 M. Brändle and G. Calzaferri, *Helv. Chim. Acta*, 1993, **76**, 924; F. Savary, J. Weber and G. Calzaferri, *J. Phys. Chem.*, 1993, **97**, 3722.

22 A. D. Berry, E. R. Corey, A. P. Hagen, A. G. MacDiarmid, F. E. Saalfeld and B. B. Wayland, *J. Am. Chem. Soc.*, 1970, **92**, 1940.

23 A. Imamura, *Mol. Phys.*, 1968, **15**, 225.

24 E. Egert and G. M. Sheldrick, *Acta Crystallogr., Sect. A*, 1985, **41**, 262.

25 G. M. Sheldrick, *Acta Crystallogr., Sect. A*, 1990, **46**, 467.

26 G. M. Sheldrick, *J. Appl. Crystallogr.*, in the press.

27 K. W. Törnroos, unpublished work.

28 A. L. Spek, PLATON-90, Vakgroep Algemene Chemie, University of Utrecht, 1990.

29 W. Hummel, J. Hauser and H. B. Bürgi, *J. Mol. Graphics*, 1990, **8**, 214.

30 E. Keller, SCHAKAL 92, A Program for the Graphic Representation of Molecular and Crystallographic Models, University of Freiburg, 1992.

31 R. Hoffmann, *J. Chem. Phys.*, 1963, **39**, 1397.

32 M. Wolfsberg and L. Helmholz, *J. Chem. Phys.*, 1952, **20**, 837.

33 G. Calzaferri, L. Forss and I. Kamber, *J. Phys. Chem.*, 1989, **93**, 5366.

34 G. Calzaferri and M. Brändle, QCMP No. 116, *QCPE Bulletin*, 1992, **12**(4), update May 1993.

35 G. Calzaferri and R. Rytz, unpublished work.